

# Investigating Mild-Stall Characteristics of NACA 4415 Airfoil

Asma S. Khan, Researcher, Bharati Vidyapeeth (Deemed to be University) College of Engineering, Pune, India, [asmaskhan70@gmail.com](mailto:asmaskhan70@gmail.com)

Pradeep V. Jadhav, Professor, Bharati Vidyapeeth (Deemed to be University) College of Engineering, Pune, India, [pvjadhav@bvucoep.edu.in](mailto:pvjadhav@bvucoep.edu.in)

Mahavir K. Beldar, Assistant Professor, Bharati Vidyapeeth (Deemed to be University) College of Engineering, Pune, India, [mkbeldar@bvucoep.edu.in](mailto:mkbeldar@bvucoep.edu.in)

**Abstract:** The paper describes the 2D CFD analysis of NACA 4415 at angles of attack from  $0^\circ$  to  $25^\circ$ . Its blunt leading edge and high cambered aft portion has influence over stall characteristics of the airfoil. The graphs of  $C_l$  and  $C_d$  vs angle of attack ( $\alpha$ ) and pressure and velocity contours at various angles of attack were plotted to study the nature of graph and air flow separation pattern respectively. The simulation was carried out on ANSYS Fluent and later graph was plotted for Lift Coefficient ( $C_l$ ), Drag Coefficient ( $C_d$ ) against  $\alpha$  respectively.

**Keywords** — Mild Stall, NACA 4415, Airfoil, Angle of Attack, 2D CFD Analysis, Lift Coefficient,  $C_l$ , Drag Coefficient,  $C_d$ , L/D ratio

## I. INTRODUCTION

Airfoils are streamlined shapes that generate lift. However, the major contributing factor is that it reduces drag to a considerable extent. Whenever, air moves over an airfoil low-pressure region is created above and a high-pressure region below it and this difference in pressure causes generation of Lift force.

Today a great interest has been developed for the use of small and medium sized UAVs. These UAVs are required to fly at low speeds and low altitudes in gusty environment. [1]. It has also become important to have long endurance of such aircrafts; therefore, there arises a need to choose a low Reynolds number airfoil which can produce high-lift and have mild stalling characteristics.

## II. CAMBER OF AN AIRFOIL

The curvature characteristics of airfoil is defined by the term 'Camber'. Line which is at equal distance from upper and lower surface of airfoil is called the 'Mean Camber Line'. Total airfoil camber is defined as the maximum distance of the mean camber line from the chord line, expressed as percent of chord. [2]

### A. Stall:

One of the characteristics of airfoils includes the shape of the lift coefficient curve up to stall angle and above that. This shape of the lift coefficient curve defines the stall behavior of the airfoil. A gentle loss in lift of airfoil, instead of an abrupt drop, beyond stall angle of attack is a safer stall behavior of an airfoil as it helps pilot to recover easily.

This stall behavior is termed as mild-stall behavior of airfoil (MS-Airfoils).

## III. MS - AIRFOILS

An airfoil having camber such that boundary layer separation starts at the aft portion of the airfoil, instead of at the leading edge i.e. nose of the airfoil, possess mild stall characteristics. [3]

Raymer, in his book, has also categorized these airfoils as "Fat" airfoils, which has round leading edge and thickness-to-chord ( $t/c$ ) ratio greater than 14%. [2] At stall angle, the boundary layer starts to separate at trailing edge and separation location moves towards leading edge as the angle of attack increases beyond that.

Alexander Nagel al explains in his paper that "High-lift, mild-stall airfoils (MS-airfoils) are single element wing sections that rely on blunt leading edge and highly cambered aft portion of the airfoil for producing mild stall characteristics at high level of maximum lift." [4] In another research work they have also concluded that "The concept of high-lift, mild stall wing relies on "blunt" leading and highly cambered aft portion of the airfoil. The combination of continuous lift build-up at forward portion of MS-airfoils and slowly creeping trailing edge separation with increasing angles of attack produce the feature of mild stall at high lift coefficients." [1]

At stall angle and post stall angles, if formation of suction peak is prevented at leading edge along with non-concave recovery of turbulent boundary layer, will develop creeping

trailing edge separation and small mild stall at high lift coefficients. [5]

#### IV. NACA 4415 AIRFOIL

One of the most common mild-stall airfoil is NACA 4415 whose geometry is as shown in Fig. 1.

According to NACA four-digit airfoil nomenclatures, the airfoil has 15%  $(t/c)_{max}$ , its maximum camber is 40% and is located at 40% of the chord length from the leading edge. This airfoil is analyzed for angles of attack from  $0^\circ$  to  $25^\circ$  to plot the graph and understand the mild stalling nature of the airfoil.

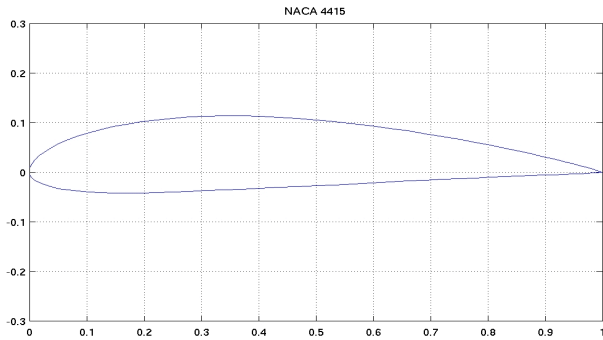


Fig. 1 Airfoil NACA 4415 [6]

#### V. 2D CFD ANALYSIS OF NACA 4415

The 2D CFD analysis was carried out on Ansys Fluent for velocity of 1.5 m/s. The geometric modeling of the airfoil was done on ANSYS Design Modeler.

Procedure Adopted:

##### A. Geometric Modeling:

The coordinates of NACA 4415 [6] were imported and an airfoil surface was generated. A C-mesh domain was created around it for air enclosure i.e. 8C radius of semicircle and 20C length of rectangle from leading edge of the airfoil. The airfoil surface was subtracted from the enclosure. See Fig. 2.

##### B. Meshing:

Meshing is performed using edge sizing and biasing in such a manner that fine mesh region is obtained around the airfoil. Later named selections were assigned for Inlet, Outlet and Airfoil as shown in Fig. (3), (4). [7]

##### C. FLUENT Setup:

Solver	Density-Based
Model	Spalart-Allmaras
Air Density	1.225 kg/m <sup>3</sup>
Kinematic Viscosity	1.7894e-5 kg/m-s
Temperature	303K
Velocity of Air at Inlet	1.5 m/s
X – Component of velocity	Cos ( $\alpha$ )
Y – Component of Velocity	Sin ( $\alpha$ )

Table 1: Fluent Setup

Then, perform Standard Initialization starting from inlet and run calculation for 500 iterations.

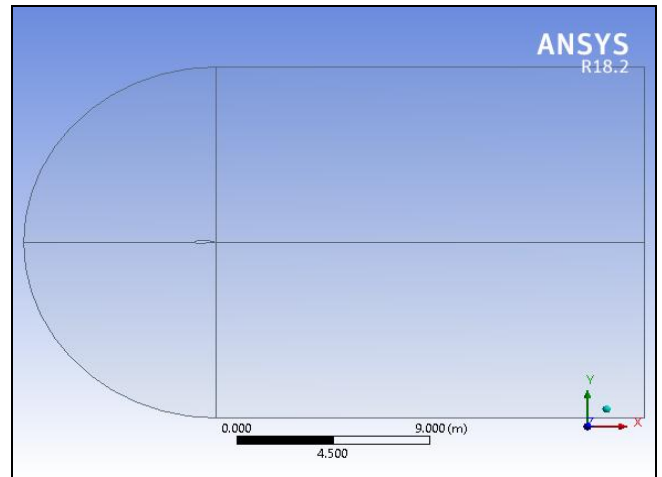


Fig. 2: Geometric Model

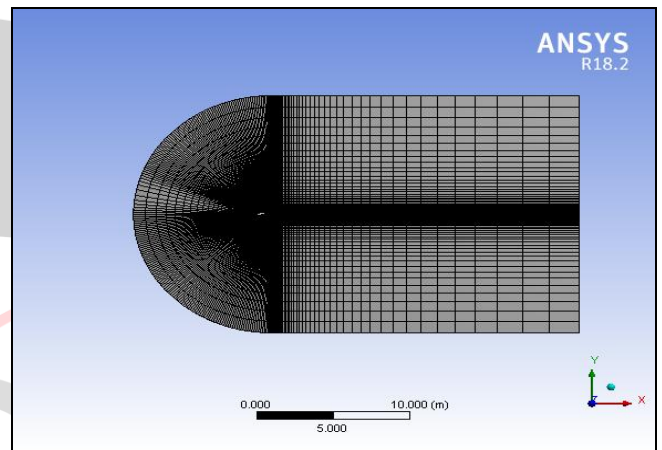


Fig. 3(a): Meshing of Airfoil Enclosure.

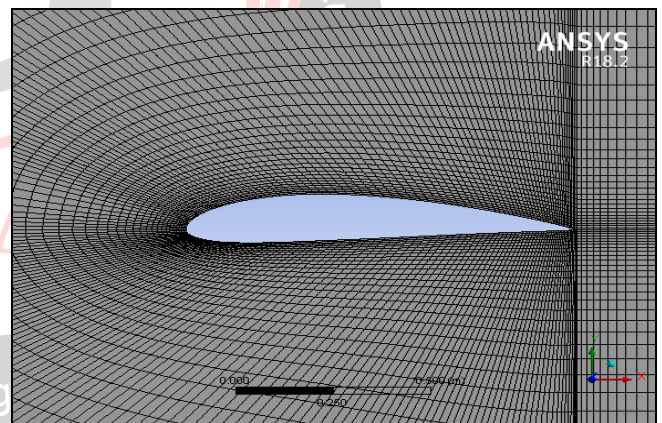


Fig. 3(b): A closer look of mesh near airfoil boundary

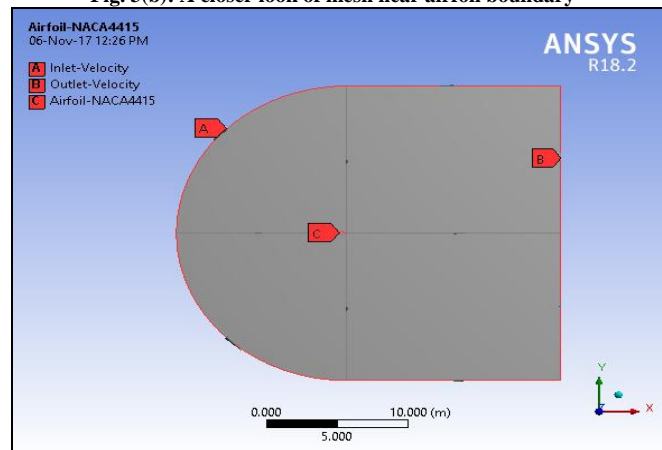


Fig. 4: Named Selection (A-Inlet, B-Outlet & C-Airfoil)

## VI. RESULTS AND DISCUSSIONS

Following Values of  $C_l$ ,  $C_d$  vs AOA ( $\alpha$ ) were calculated by performing 2D CFD Analysis on ANSYS:

AOA	$C_l$	$C_d$
0	0.52134	0.005784
1	0.63517	0.00605
2	0.74683	0.006584
3	0.85479	0.007369
4	0.96078	0.008405
5	1.068	0.009601
6	1.1683	0.011012
7	1.268	0.012694
8	1.3706	0.01498
9	1.4588	0.017515
10	1.543	0.020463
11	1.6176	0.02383
12	1.6754	0.027653
13	1.7128	0.032251
14	1.7215	0.038615
15	1.6905	0.047999
16	1.6234	0.063196
17	1.5178	0.084846
18	1.4205	0.11047
19	1.3451	0.13662
20	1.286	0.16308
21	1.2356	0.1918
22	1.1907	0.22064
23	1.1584	0.2503
24	1.1288	0.27776
25	1.1139	0.3076

Thus, the  $C_l$  and  $C_d$  graphs obtained respectively are as follows:

### i. $C_l$ vs $\alpha$ Graph:

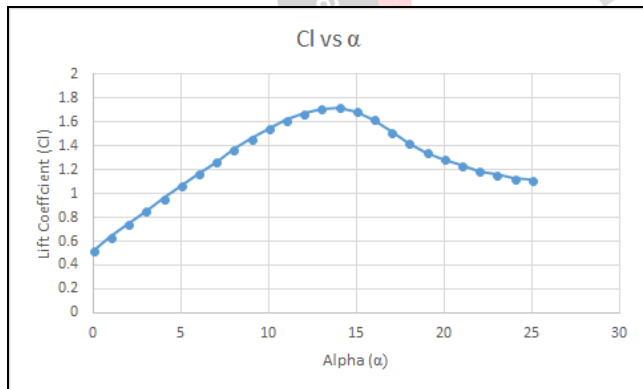


Fig 5:  $C_l$  vs  $\alpha$  Graph from results obtained in CFD Analysis

It is observed from the graph that maximum lift occurs at 14° angle of attack beyond flow separation increases causing a gentle decrease in lift.

### ii. $C_d$ vs $\alpha$ Graph:

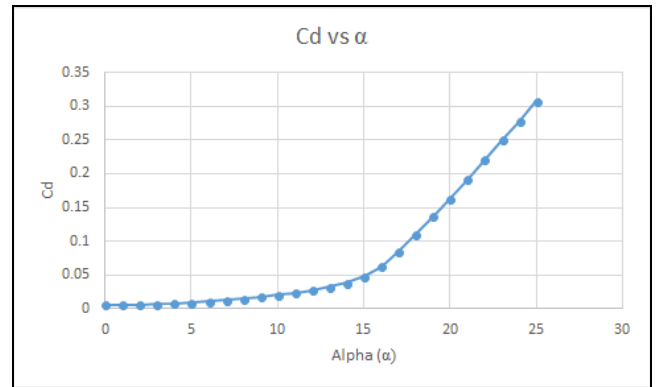


Fig. 6:  $C_d$  vs  $\alpha$  Graph from results obtained in CFD Analysis

$C_d$  value also gradually increases after stall angle of attack i.e. 14°. This sudden increase in drag is due to occurrence of flow separation beyond 14° of angle of attack.

### iii. $C_l/C_d$ vs $\alpha$ Graph:

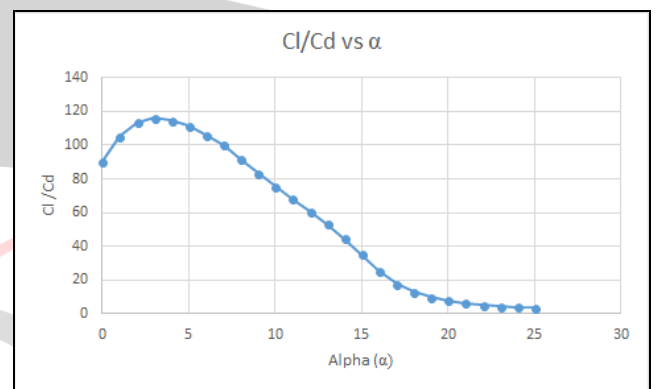


Fig. 7:  $C_l/C_d$  vs  $\alpha$  Graph from results obtained in CFD Analysis

Maximum  $C_l/C_d$  is obtained at 3° angle of attack after which the graph falls gradually. A fair L/D value of 116 is obtained.

### iv. Pressure Contours at 8°, 14° and 20° of Angle of Attack:

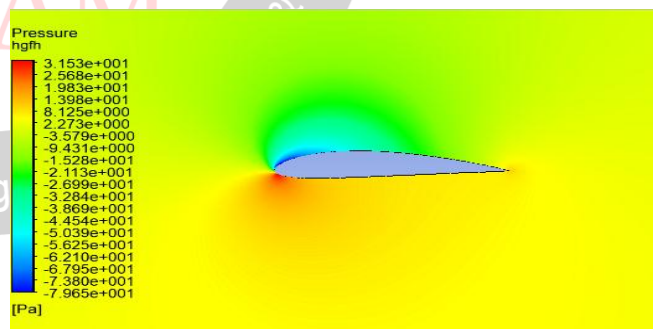


Fig. 9 (a): Pressure Contour at 8° angle of attack

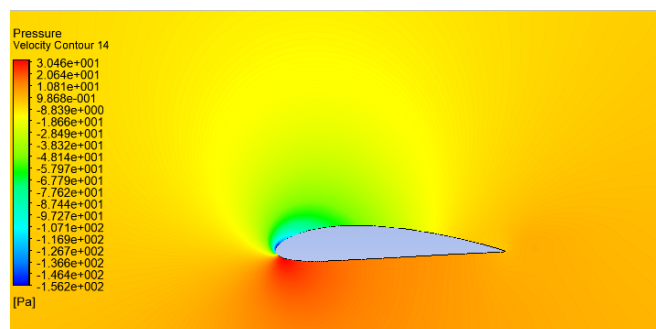


Fig. 9 (b): Pressure Contour at 14° angle of attack

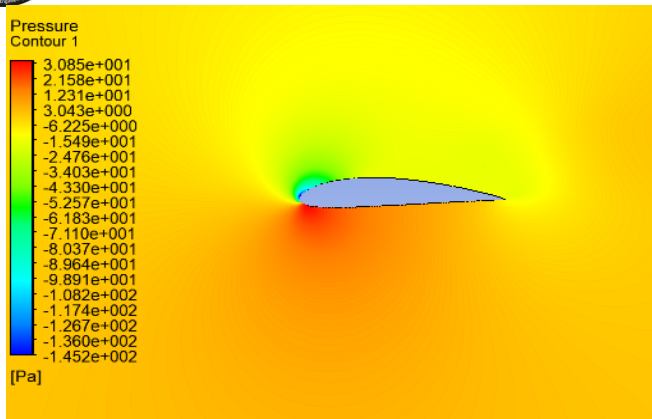


Fig. 9 (c): Pressure Contour at 20° angle of attack

It can be observed as the angle of attack increases beyond 14° very high-pressure region is generated below the airfoil causing a shift in its centre of pressure.

v. Velocity Contours at 8°, 14° and 20° of Angle of Attack:

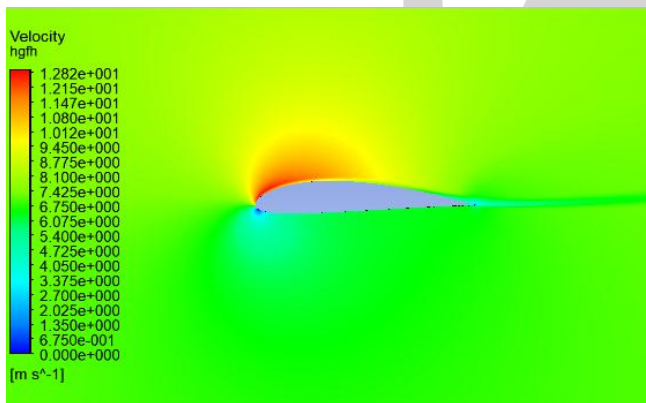


Fig. 10 (a): Velocity Contour at 8° Angle of Attack

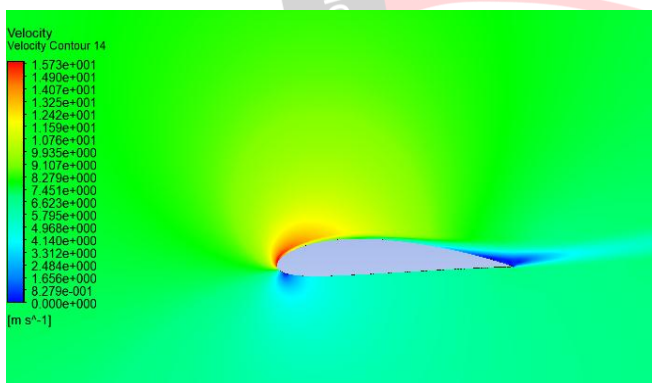


Fig. 10 (b): Velocity Contour at 14° Angle of Attack

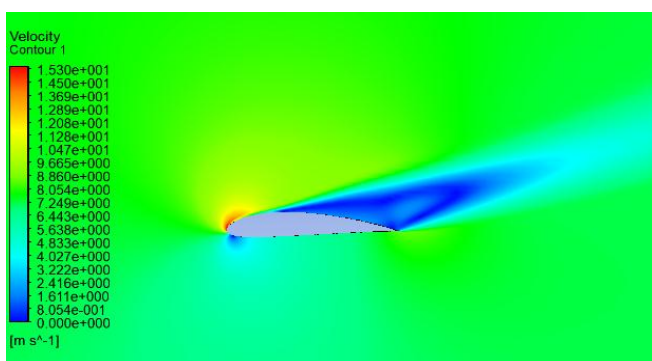


Fig. 10 (c): Velocity Contour at 20° Angle of Attack

From the velocity contours it is evident that, the flow separation beyond critical angle of attack i.e. 14° starts at the aft portion of the airfoil and increases further as the angle of attack increases.

## VII. CONCLUSION

The  $C_l$  vs  $\alpha$  graph of airfoil NACA 4415 shows that the airfoil has mild stall characteristics. This is due separation of flow at aft portion of the airfoil due to its blunt leading edge and a highly cambered aft portion. The flow separation increases beyond causing a gentle decrease in lift instead of an abrupt stall behavior.

## REFERENCES

- [1] Nagel, Alexander, and Misha Shepshelovich. "The concept of High-Lift, Mild Stall Wing." In *24th International Congress of the Aeronautical Sciences, Yohogama, Japan, 29August-03 September. 2004.*
- [2] Raymer, Daniel P. "Aircraft Design: A conceptual approach, AIAA Education series." *Washington, DC (1992).*
- [3] Sadraey, Mohammad. "Wing Design." *Sep-2012.[Online]. Available: http://faculty.dwc.edu/sadraey (2012).*
- [4] Nagel, Alexander, and Misha Shepshelovich. "Development of high-lift UAV wings." In *24th AIAA Applied Aerodynamics Conference. 2006.*
- [5] Koss, D., M. Steinbuch, and M. Shepshelovich. "Design and experimental evaluation of a high-lift, mild-stall airfoil." In *12th AIAA Applied Aerodynamics Conference. 1994.*
- [6] University of Illinois at Urbana Champaign, "UIUC Airfoil Coordinates Database", Department of Aerospace Engineering  
Available at:  
[http://m-selig.ae.illinois.edu/ads/coord\\_database.html](http://m-selig.ae.illinois.edu/ads/coord_database.html)
- [7] Bagade, Aditya, Changki Mo, and Abdelhamid Mazher. "Degradation of Power Generation Performance due to Effects of Various Ice Shapes and Accretions on Wind Turbine Blades." *Energy Research Journal* 6, no. 2 (2015): 42.